A NON-EMPIRICAL RELATIVE PERMEABILITY MODEL FOR GAS AND WATER FLOW IN HYDRATE-BEARING SEDIMENTS

Harpreet Singh[1*], Evgeniy M. Myshakin,[1,2] Yongkoo Seol[1]

[1]*National Energy Technology Laboratory, Morgantown, WV, USA*
[2]*AECOM, 626 Cochrans Mill Road, Pittsburgh, PA*

* Corresponding author: harpreet.singh@netl.doe.gov

ABSTRACT

At present, there are two types of relative permeability models that are used to model gas production from hydrate-bearing sediments, i) fully empirical parameter fitting models (van Genuchten, Brooks Corey etc.), ii) Kozeny-Carman and capillary tube based models that assume only water as the mobile phase. A relative permeability model without the limitations of these two families of models, and that depends on characteristics of both fluids and host porous media with hydrates is required to accurately represent relative permeability of both gas and water in hydrate reservoirs. This study proposes an analytical model based on fundamental principles of multiphase fluid flow to estimate relative permeability of both gas and water as a function of three phase saturations (hydrate, gas, water) and fluid properties.

INTRODUCTION

Review of the methane hydrate literature reveals that relative permeability of the methane hydrate bearing sediments remains a topic of curve fitting exercise that also requires obtaining laboratory data of relative permeability for various saturations of hydrates. Clearly, in addition to being an expensive exercise, the relative permeability obtained from curve fitting the laboratory results is applicable only to that particular hydrate medium. Moreover, considering hydrates in multiphase flow laboratory experiments is relatively difficult, and therefore, there are very few water relative permeability data [1]–[4] for hydrate bearing sediments.

At present, there are two types of relative permeability models that are used to model gas production from hydrate-bearing sediments, i) fully empirical parameter fitting models (van Genuchten, Brooks Corey etc.), ii) Kozeny-Carman and capillary tube based models that assume only water as the fluid phase. In this paper, we propose a new relative permeability model of hydrate that is free of empirical parameters by using Navier Stokes equations for water and gas as two mobile phases and hydrate as an immobile phase. We call this relative permeability model as *Nonempirical Relative Permeability* (NRP). The three novelties of the NRP model that make it better suited over other relative permeability models for hydrate are:

(1) It does away with the shortcomings of empirical models that require curve fitting on laboratory data, which is a relatively expensive and time consuming exercise.
(2) It accounts for two mobile phases of gas and water in addition to one immobile phase of hydrate.
(3) It is derived on fundamental principles of multiphase fluid flow, hence, it can be used to obtain important physical parameters (for e.g. irreducible water saturation) by history matching laboratory data.

Table 1: Equations and empirical parameters of hydrate relative permeability models for comparison with the NRP model

Model	Equation	Empirical Parameters	Description of Parameters
U. of Tokyo Model [5]	$k_{rw} = (1 - S_h)^N$	N	Permeability reduction exponent due to accumulation of hydrates
Kozeny Grain Model [6]	$k_{rw} = \frac{(1-S_h)^{n+2}}{(1-\sqrt{S_h})^2}; k_{rw} = (1 - S_h)^{n+1}$	n	Archie saturation exponent that models the presence of hydrates
Parallel Capillary Model [6]	$k_{rw} = 1 - S_h^2 + \frac{2(1-S_h)^2}{\log(S_h)}; k_{rw} = (1 - S_h)^2$	None	None
Daigle Model [7]	$k_r = \left[\frac{\beta-\phi+\phi(S_\chi-p_c)}{\beta-\phi p_c}\right]^{\frac{D}{3-D}} \times \left[\frac{S_w-p_c}{S_\chi-p_c}\right]^2$	β, p_c, D	Scaling factor in fractal model, percolation threshold, and fractal dimension, respectively.
NRP (this study)	k_{rg} from equation (52) [=(27), (44)] and k_{rw} from equation (53) [=(28), (45)]	None	None

The theory and modeling used in deriving NRP is explained in the next section. In the results section, we validate our model by comparing against the relative permeability data of hydrate available in the literature, followed by a comparison of predictions from our model with two other popular models and the most recent model published in the literature. We then use our model to predict relative permeability results in presence of three phases: hydrate, gas and water. Finally, we summarize the contribution of the proposed model and suggest some recommendations to predict relative permeability for multiphase flow in hydrate-bearing sediments.

2. THEORY AND MODELING

The relative permeability of a particular mobile phase in the porous media is the ratio of the flow rate of that phase at a given saturation to the flow rate with 100% saturation under similar operating conditions and medium properties. Relative permeability is typically obtained from laboratory experiments by varying in-situ fluid saturation and measuring the corresponding changes in permeability to that fluid. Although, fluid flow inside a porous medium is a complex function of fluid saturations, fluid properties, heterogeneity in rock properties, etc., simplifying assumptions have been used by several researchers to reliably model the fluid flow in porous media. We use the same approach to obtain a simplified model of relative permeability of hydrate bearing sediments by solving Navier Stokes equations for a system of three phases (hydrate, gas, water). Solutions of Navier Stokes equations are used to obtain flux of each fluid at a given saturation and that flux is used in the formulation of Darcy's law to obtain the relative permeability of each phase. Below, we describe the approach to obtain relative permeability of each phase starting from their flow model. After we have described the general approach to obtain relative permeabilities, we consider two types of hydrate growth pattern and find appropriate relative permeabilities for those two types of hydrate growth in the porous medium.

2.1. General Approach

2.1.1. Assumptions

Following assumptions are made to simplify the flow system:

(1) Porous medium consists of three phases (hydrate, gas, water) that are uniformly distributed, with the wetting phase being water and non-wetting phase being gas.
(2) The porous medium is composed of a bundle of cylindrical capillary tubes of uniform cross-sections.
(3) The fluid flow is isothermal, laminar, and horizontal flow with no effect of gravity.
(4) The fluid flow is driven by convection (pressure difference) only and there is no interaction between different phases.
(5) Capillary pressure between non-wetting phase and wetting phase is negligible.
(6) The flow for gas and water is fully developed and at steady state.

2.1.2. Flow equation

Under above conditions, the momentum equation for gas flow and water flow can be described by steady state Navier Stokes equation in a capillary tube of radius r as follow:

$$\mu\left[\frac{1}{r}\frac{\partial}{\partial r}\left(r\frac{\partial v}{\partial r}\right)\right]=\frac{\partial P}{\partial x} \quad (1)$$

Here, $\frac{\partial P}{\partial x}$ is the pressure gradient along the horizontal direction of the flow, v is the fluid velocity, and μ is the fluid viscosity. If $\frac{\partial P}{\partial x}$ =constant= ∇P, then above equation can be written as following:

$$\mu\left[\frac{1}{r}\frac{\partial}{\partial r}\left(r\frac{\partial v}{\partial r}\right)\right]=\nabla P \quad (2)$$

2.1.3. Volumetric flow rates

The above equation is integrated twice analytically to obtain velocity for gas (non-wetting) and water (wetting) phases, respectively:

$$v_g=\frac{\nabla P_g}{\mu_g}\frac{r^2}{4}+c_1\ln(r)+c_2 \quad (3)$$

$$v_w=\frac{\nabla P_w}{\mu_w}\frac{r^2}{4}+c_3\ln(r)+c_4 \quad (4)$$

If $c_g=\frac{\nabla P_g}{4\mu_g},\ c_w=\frac{\nabla P_w}{4\mu_w},\ \alpha=\frac{\mu_g}{\mu_w}$ (5)

$$v_g=c_g r^2+c_1\ln(r)+c_2 \quad (6)$$

$$v_w=c_w r^2+c_3\ln(r)+c_4 \quad (7)$$

The velocity distribution of each phase is obtained by solving for constants of integration for appropriate boundary conditions of the system that will depend on the growth pattern of the hydrate. Once the velocity is known, the volumetric flux of gas and water is estimated by integrating the velocity of each phase over its flowing area, i.e.:

$$q_g=\int_r^{r_g} v_g.(2\pi r dr) \quad (8)$$

$$q_w=\int_r^{r_w} v_w.(2\pi r dr) \quad (9)$$

2.1.4. Relative permeabilities

After we obtain the volumetric flow rate (q) for each phase as a function of its saturation, we can substitute them in Darcy's law to obtain the relative permeability of that phase as following:

$$q_i = -\frac{k k_{ri} A_i}{\mu} \nabla P \tag{10}$$

$$\Rightarrow k_{ri} = -\frac{(q_i/A_i)\ \mu_i}{k \nabla P} \tag{11}$$

Here, k is the absolute permeability of the porous medium, k_{ri} is the relative permeability of each phase $(= g, w)$, μ_i is the viscosity of phase i, A_i is the cross-sectional area of flow occupied by phase i, and ∇P is the pressure gradient in the direction of flow.

The term (q_i/A_i) is the superficial velocity (or Darcy velocity), which is a hypothetical velocity in multiphase flows in porous media that assumes the given fluid phase is the only one flowing. However, if we know the absolute permeability of the porous medium for a given shape of pore, then one can find the relative permeability of each phase as following:

$$k_{rg} = -\frac{(q_g/A_g)\ \mu_g}{k \nabla P} \tag{12}$$

$$k_{rw} = -\frac{(q_w/A_w)\mu_w}{k \nabla P} \tag{13}$$

We use the approach described above to find relative permeability of hydrate bearing sediments for two different types of hydrate growth patterns – i) hydrates occupying pore center, and ii) hydrates coating pore wall, respectively.

2.2. Pore Filling (PF) Hydrates

The most commonly assumed hydrate growth pattern is the hydrate occupying the center of the pore, also known as pore filling hydrates. In the case of a cylindrical pore, this type of hydrate growth leaves an open annulus around it where gas and water can flow. This type of flow scenario is shown by a sketch in Figure 1, where water is the wetting phase lying closer to the pore walls while the gas is the non-wetting phase that lies closer to the pore center. This sketch also shows an irreducible layer of water around the pore wall that is immobile, but forms the part of overall water saturation. To avoid complexity, we do not consider any irreducible gas saturation.

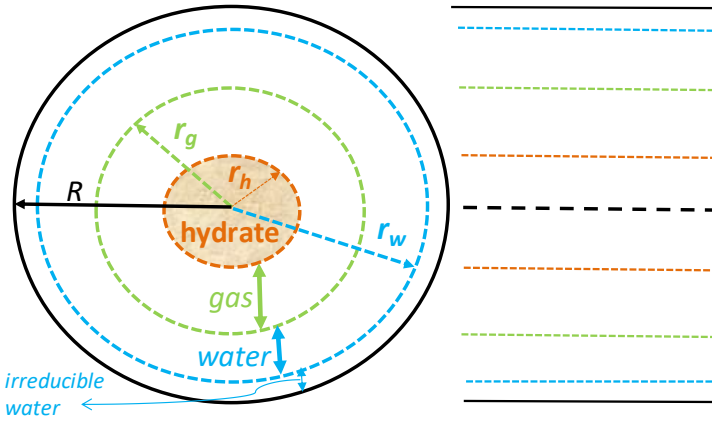

Figure 1: Cross-sections of the capillary shaped pore with hydrate occupying the pore center

The velocity profiles of gas and water obtained by analytically integrating the momentum equation for gas flow and water flow, respectively, are solved for the following boundary conditions specific to the system of hydrates occupying pore center. The boundary conditions are set by the symmetry of the cylindrical pore shape and no-slip velocity at the layer of the irreducible water and the surface of hydrates. Besides the conditions of zero velocity at the static surface, continuity of flow velocity and shear stress are needed at the interface of two fluids.

2.2.1. Boundary conditions:

$$v_g = 0 \text{ at } r = r_h \tag{14}$$

$$v_g = v_w \text{ at } r = r_g \tag{15}$$

$$\tau_g = \tau_w \text{ at } r = r_g \Rightarrow \mu_g \frac{\partial v_g}{\partial r} = \mu_w \frac{\partial v_w}{\partial r} \text{ at } r = r_g \tag{16}$$

$$v_w = 0 \text{ at } r = r_w \tag{17}$$

Using the above boundary conditions, we solve for a system of 4 equations to find the velocity distribution of each phase for its given saturation. The equations obtained on substituting the above boundary conditions (B.C.s) with given saturations of each phase are shown in Appendix A.1. We use those velocity distributions to obtain volumetric flow rates of each phase along its flow area.

2.2.2. Flow rates:

Integrating the flow velocity of gas and water along their flow areas to obtain the volumetric flow rates as follow:

$$q_g = \int_{r_h}^{r_g} v_g.(2\pi r dr) \tag{18}$$

$$q_w = \int_{r_g}^{r_w} v_w.(2\pi r dr) \tag{19}$$

$$q_g = \frac{\pi \nabla P}{8\mu_g}\left[-\left(r_g^4 - r_h^4\right) + 4\left\{\frac{r_g^2(1-\alpha)+R^2\alpha-r_h^2}{(1-\alpha)\ln(r_g)+\alpha\ln(R)-\ln(r_h)}\right\}\left\{\frac{r_g^2\ln(r_g)-r_h^2\ln(r_h)}{2} - \frac{(r_g^2-r_h^2)}{4}\right\} + 2\left\{\frac{(1-\alpha)[r_h^2\ln(r_g)-r_g^2\ln(r_h)]+\alpha[r_h^2\ln(R)-R^2\ln(r_h)]}{(1-\alpha)\ln(r_g)+\alpha\ln(R)-\ln(r_h)}\right\}\left(r_g^2 - r_h^2\right)\right] \tag{20}$$

$$q_w = \frac{\pi \nabla P}{8\mu_w}\left[-\left(R^4 - r_g^4\right) + 4\left\{\frac{r_g^2(1-\alpha)+R^2\alpha-r_h^2}{(1-\alpha)\ln(r_g)+\alpha\ln(R)-\ln(r_h)}\right\}\left\{\frac{R^2\ln(R)-r_g^2\ln(r_g)}{2} - \frac{(R^2-r_g^2)}{4}\right\} + 2\left\{\frac{(1-\alpha)[R^2\ln(r_g)-r_g^2\ln(R)]-R^2\ln(r_h)+r_h^2\ln(R)}{(1-\alpha)\ln(r_g)+\alpha\ln(R)-\ln(r_h)}\right\}\left(R^2 - r_g^2\right)\right] \tag{21}$$

2.2.3. Relative permeabilities of gas and water:

The above obtained volumetric flow rates for each phase are substituted in Darcy's law to obtain their corresponding NRP as following.

$$k_{rg} = -\frac{(q_g/A_g)\ \mu_g}{k\nabla P} \tag{22}$$

$$k_{rw} = -\frac{(q_w/A_w)\mu_w}{k\nabla P} \tag{23}$$

For a cylindrical pore of radius R, the absolute permeability is given as:

$$k = R^2/8 \tag{24}$$

The flow area for gas and water in the case of hydrate occupying the pore center are:

$$A_g = \pi(r_g^2 - r_h^2) \tag{25}$$

$$A_w = \pi(r_w^2 - r_g^2) \tag{26}$$

Substituting the volumetric flow rate and cross sectional flow area in above equations yield the final NRP of gas and water for pore filling hydrates as following:

$$(k_{rg})_{pf} = \left\{\frac{1}{R^2(r_g^2-r_h^2)}\right\}.\left[-(r_g^4 - r_h^4) + 4\left\{\frac{r_g^2(1-\alpha)+R^2\alpha-r_h^2}{(1-\alpha)\ln(r_g)+\alpha\ln(R)-\ln(r_h)}\right\}\left\{\frac{r_g^2\ln(r_g)-r_h^2\ln(r_h)}{2} - \frac{(r_g^2-r_h^2)}{4}\right\} + 2\left\{\frac{(1-\alpha)[r_h^2\ln(r_g)-r_g^2\ln(r_h)]+\alpha[r_h^2\ln(R)-R^2\ln(r_h)]}{(1-\alpha)\ln(r_g)+\alpha\ln(R)-\ln(r_h)}\right\}(r_g^2 - r_h^2)\right] \quad (27)$$

$$(k_{rw})_{pf} = \left\{\frac{1}{R^2(r_w^2-r_g^2)}\right\}.\left[-(R^4 - r_g^4) + 4\left\{\frac{r_g^2(1-\alpha)+R^2\alpha-r_h^2}{(1-\alpha)\ln(r_g)+\alpha\ln(R)-\ln(r_h)}\right\}\left\{\frac{R^2\ln(R)-r_g^2\ln(r_g)}{2} - \frac{(R^2-r_g^2)}{4}\right\} + 2\left\{\frac{(1-\alpha)[R^2\ln(r_g)-r_g^2\ln(R)]-R^2\ln(r_h)+r_h^2\ln(R)}{(1-\alpha)\ln(r_g)+\alpha\ln(R)-\ln(r_h)}\right\}(R^2 - r_g^2)\right] \quad (28)$$

The radius of flow areas for gas (r_g) and water (r_w) in above expressions of relative permeabilities can be expressed in terms of gas saturation (S_g) and water saturation (S_w), respectively, as shown in Appendix A.1.

2.3. Wall Coating (WC) Hydrates

Figure 2 shows a sketch of hydrate coating the pore wall, where water and gas flow in the center of the pore. Here, water as the wetting phase is placed closer to the pore walls and the gas as the non-wetting phase is placed closer to the pore center. This sketch also shows an irreducible layer of water around the hydrate surface that is immobile, but forms the part of overall water saturation. Similar to the earlier case, we do not consider any irreducible gas saturation to avoid complexity.

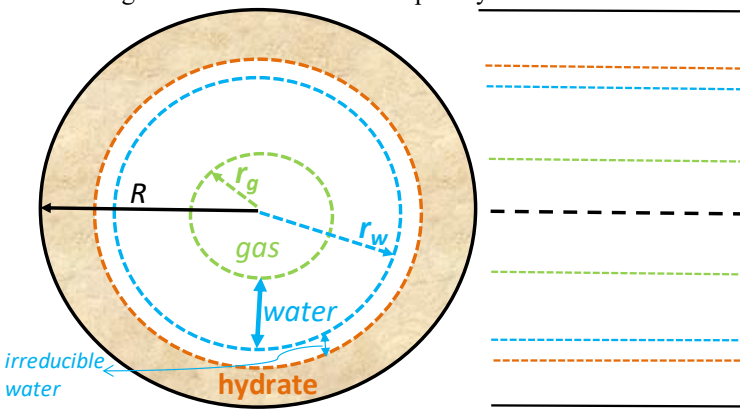

Figure 2: Cross-sections of the capillary shaped pore with hydrate coating the pore wall

The velocity profiles of gas and water obtained by analytically integrating the momentum equation for gas flow and water flow, respectively, are solved for the following boundary conditions specific to the system of hydrates coating pore wall. The boundary conditions are set by the symmetry of the cylindrical pore shape and no-slip velocity at the layer of the irreducible water. Besides the conditions of zero velocity at the static surface, continuity of flow velocity and shear stress are needed at the interface of two fluids.

2.3.1. Boundary conditions:

$$\frac{\partial v_g}{\partial r} = 0 \text{ at } r = 0 \quad (29)$$

$$v_g = v_w \text{ at } r = r_g \quad (30)$$

$$\tau_g = \tau_w \text{ at } r = r_g \Rightarrow \mu_g \frac{\partial v_g}{\partial r} = \mu_w \frac{\partial v_w}{\partial r} \text{ at } r = r_g \quad (31)$$

$$v_w = 0 \text{ at } r = r_w \quad (32)$$

Using the above boundary conditions, we solve for a system of 4 equations to find the velocity distribution of each phase for its given saturation. The equations obtained on substituting the above B.C.s with given saturations of each phase are shown in Appendix A.2. We use those velocity distributions to obtain volumetric flow rates of each phase along its flow area.

2.3.2. Flow rates:

Integrating the flow velocity of gas and water along their flow areas to obtain the volumetric flow rates as follow:

$$q_g = \int_0^{r_g} v_g.(2\pi r dr) \quad (33)$$

$$q_w = \int_{r_g}^{r_w} v_w.(2\pi r dr) \quad (34)$$

$$q_g = \frac{\pi \nabla P r_g^4}{8\mu_g}\left[2\alpha\left(1 - \frac{r_w^2}{r_g^2}\right) - 1\right] \quad (35)$$

$$q_g = \frac{\pi \nabla P R^4}{8\mu_g}\left[(2\alpha - 1)S_g^2 + 2\alpha S_g S_h - 2\alpha S_g + 2\alpha S_g S_{wr}\right] \quad (36)$$

$$q_w = \frac{\pi \nabla P}{8\mu_w}\left[-\left(r_w^2 - r_g^2\right)^2\right] \quad (37)$$

$$q_w = \frac{\pi \nabla P R^4}{8\mu_w}\left[-\left(1 - S_g - S_h - S_{wr}\right)^2\right] \quad (38)$$

2.3.3. Relative permeabilities of gas and water:

The above obtained volumetric flow rates for each phase are substituted in Darcy's law to obtain their corresponding NRP as following.

$$k_{rg} = -\frac{(q_g/A_g)\ \mu_g}{k\nabla P} \quad (39)$$

$$k_{rw} = -\frac{(q_w/A_w)\mu_w}{k\nabla P} \quad (40)$$

For a porous medium with cylindrical pores of radius R, the absolute permeability is given as:

$$k = R^2/8 \quad (41)$$

The flow area for gas and water in the case of hydrate coating the pore wall are:

$$A_g = \pi r_g^2 \quad (42)$$

$$A_w = \pi(r_w^2 - r_g^2) \quad (43)$$

Substituting the volumetric flow rate and cross sectional flow area in above equations yield the final NRP of gas and water for wall coating hydrates as following:

$$\left(k_{rg}\right)_{wc} = \left(\frac{r_g^2}{R^2}\right).\left[2\alpha\left(1 - \frac{r_w^2}{r_g^2}\right) - 1\right] \quad (44)$$

$$(k_{rw})_{wc} = \left[-\frac{(r_w^2 - r_g^2)^2}{R^2(r_w^2 - r_g^2)}\right] \quad (45)$$

The radius of flow areas for gas (r_g) and water (r_w) in above expressions of relative permeabilities can be expressed in terms of gas saturation (S_g) and water saturation (S_w), respectively, as shown in Appendix A.2.

2.4. Relative Permeability for Variably Shaped Pores

While the ideal capillary shaped pore space helps simplify the flow system, the porous media is in general a system of different and irregular pore shapes with non-linearly varying length. A general approach to

account for different pore shapes in capillary flow as proposed by different authors [8], [9] is to modify the characteristic length of the ideal pore shape by multiplying with a correction factor (β) that accounts for different pore shapes. The value of this correction factor for cylindrical, square, and an equilateral triangle geometry [8] is found to be $\beta = 1,\ 1.094$ and 1.186, respectively. Therefore, the relative permeability for the two hydrate growth pattern can be obtained different pore shapes by generalizing the absolute permeability of the cylindrical pore to any general pore shape as follow:

$$k = (\beta R)^2/8 \tag{46}$$

$$k_{rg} = \frac{(k_{rg})_{cylindrical}}{\beta^2} \tag{47}$$

$$k_{rw} = \frac{(k_{rw})_{cylindrical}}{\beta^2} \tag{48}$$

Therefore, the relative permeability of gas (or water) would decrease by a factor of 1.094^2 and 1.186^2 if the pore were to be of square shaped and equilateral triangle shaped, respectively. The effect of tortuous pore shapes can be accounted by replacing the straight length in $\nabla P\ (= \Delta P/L)$ with the actual tortuous length (L_a) as $\Delta P/L_a$. One of the assumptions used in above statement is that the gas and water flow in variably shaped pores can be approximated by a circular cross section.

2.4. A Generalized Non-Empirical Relative Permeability Model for Hydrates

While relative permeability for a single idealized pattern of hydrate growth is useful for theoretical studies, the actual hydrate growth in the porous media is generally more complicated and not well understood. However, field data from Nankai Trough in terms of well-log responses [10] shown by Figure 3 for the growth pattern of marine hydrate sediments (liquid-water-wet) indicates that gas hydrates predominantly fill the pores or they coat the pore walls to a much smaller extent without any cementing. Even though the data from [10] (as presented in Figure 3) is at field scale, the specific scale of each data point corresponds to the resolution of well-log that measures acoustic velocity, which is typically about 0.5 m [11]. Most of the hydrate growth pattern observed at laboratory scale is at much smaller scale, and although we may observe many different growth patterns that do not correlate in proportion to the field observations, a better approach of assigning the shapes to hydrate growth pattern would be to measure the representative elementary volumes [12]–[14] for each shape and then finding their relative proportion in the porous medium.

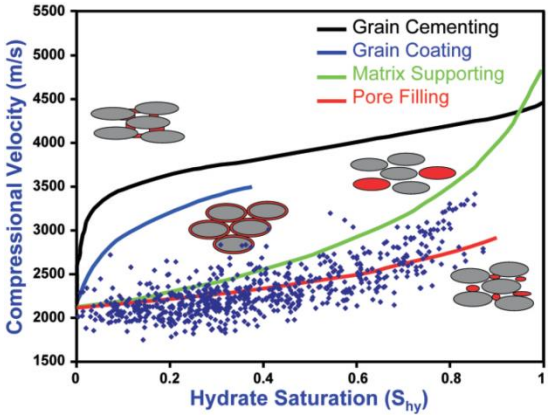

Figure 3: Field data (from [10]) in terms of compressional velocity showing the growth pattern of hydrates as either pore filling (predominantly) or coat the pore walls (much lesser extent)

We use the above observation as a practical guidance to develop a generalized form of the NRP, i.e. we assume that the total saturation of hydrates in a porous media is composed of some fraction (x_{pf}) that is

pore filling and the remaining fraction $(1 - x_{pf})$ that is coating the pore walls. Additionally, we also use the fact that most reservoirs have nearly log-normal permeability distributions [15], [16]. To develop a generalized NRP model with the above field-based practical observations, we use two mathematical properties, i.e. i) taking logarithm of a log-normal distribution produces a Gaussian (normal) distribution, and ii) the sum of independent normal distributions is a normal distribution [17], [18]. In terms of permeability, it means that the relative permeability due to each hydrate growth pattern contributes to the effective relative permeability in the porous medium, where this effective relative permeability is the statistical sum of the relative permeability from each growth pattern of hydrates.

$$\ln(k_{ri})_{eff} = x_{pf} \ln\left\{\frac{(k_{ri})_{pf}}{\beta^2}\right\} + (1 - x_{pf}) \ln\left\{\frac{(k_{ri})_{wc}}{\beta^2}\right\} \quad (49)$$

$$\ln(k_{ri})_{eff} = \ln\left[\left\{\frac{(k_{ri})_{pf}}{\beta^2}\right\}^{x_{pf}} \times \left\{\frac{(k_{ri})_{wc}}{\beta^2}\right\}^{1-x_{pf}}\right] \quad (50)$$

$$(k_{ri})_{eff} = \left[\left\{\frac{(k_{ri})_{pf}}{\beta^2}\right\}^{x_{pf}} \times \left\{\frac{(k_{ri})_{wc}}{\beta^2}\right\}^{1-x_{pf}}\right] \quad (51)$$

Using the formulation of equation (51), relative permeability for gas and water for variable shaped pores and in presence of hydrates that partially occupy pore centers and partially coat the pore walls is given as following:

$$\left(k_{rg}\right)_{eff} = \left[\left\{\frac{(k_{rg})_{pf}}{\beta^2}\right\}^{x_{pf}} \times \left\{\frac{(k_{rg})_{wc}}{\beta^2}\right\}^{1-x_{pf}}\right] \quad (52)$$

$$(k_{rw})_{eff} = \left[\left\{\frac{(k_{rw})_{pf}}{\beta^2}\right\}^{x_{pf}} \times \left\{\frac{(k_{rw})_{wc}}{\beta^2}\right\}^{1-x_{pf}}\right] \quad (53)$$

The expressions $\left(k_{rg}\right)_{pf}$, $\left(k_{rg}\right)_{wc}$, $(k_{rw})_{pf}$, and $(k_{rw})_{wc}$ used in the general NRP model for gas and water given by equation (52) and (53), respectively, can be substituted from equations (27), (44), (28), and (45), respectively.

3. RESULTS

Model Validation

We validate our model using experimental data as well as verify it by comparing against the results from two popular models and a most recent model proposed for hydrate relative permeability.

3.1.Validation with experimental data

We use four different experimental data sets to compare them against the predictions from our model. The experimental data used for validation is described in Table 2, which includes the source, the rock sample, initial pressure/temperature conditions, and the experimental method used.

Table 2: Details of experimental data used to validate the NRP model

Data Source	Rock sample	Initial P/T Conditions	Experimental Method
Delli and Grazic (2014) [1]	Ottawa sand pack containing CO2 hydrate	3 C, 3 MPa	After forming hydrate under constant volume conditions, remaining CO2 was displaced by helium and permeability measured by steady-state flow of water
Johnson et al.	Unconsolidated	2-4 C,	After forming hydrate under constant volume

(2011) [2]	samples from Mount Elbert test well, Alaska North Slope	6.9 MPa	conditions, remaining methane was displaced by brine and permeability measured by steady-state method
Kumar et al. (2010) [3]	Glass bead pack containing CO2 hydrate	4 C, 2.76 MPa	After forming hydrate under constant volume conditions, permeability measured by steady-state method
Liang et al. (2011) [4]	Sand pack containing methane hydrate	0.5 C, 3 MPa	After forming hydrate under constant volume conditions, permeability measured by steady-state method

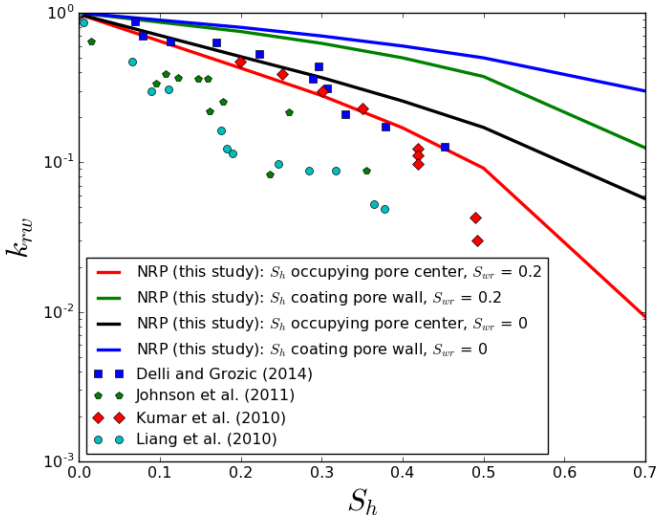

Figure 4: Comparison of water relative permeability vs. hydrate saturation experimental datasets from four studies with the predictions from NRP (this study)

Figure 4 shows a comparison of our model with the experimental data from four different studies. The relative permeability from each of these experiments has a considerable noise in their data, but our model is able to find a close match with non-zero irreducible water saturation when the hydrates occupy pore center. This match can be improved further by considering a combination of hydrate growth pattern partially as pore center and partially as wall coating. The effect of considering such combination of hydrate growth on relative permeability as estimated by NRP can be seen in results shown in Appendix B. It should be noted that some authors (specifically from non-petroleum field) refer the curves shown in Figure 4 as 'permeability reduction curve', however, such terminology is not used in petroleum engineering community where the term 'relative permeability' is used specifically for multiphase flow. A more appropriate term would be reduction in relative permeability.

3.2.Validation with model comparison

We use three different relative permeability models for hydrate bearing sediments to compare them against the predictions from our model. The models are described in Table 3, which includes the type of model, its description with pros and cons. The first two models are the two most popular models used to estimate

relative permeability for hydrate bearing sediments, where the first model is purely empirical model, and the second model is based on single phase flux through capillary type pores. The third model is the most recently proposed model that includes three different empirical parameters and is based on critical path analysis.

Table 3: Comparison of different relative permeability models for hydrate with our NRP model

Model	Description	Pros	Cons
U. of Tokyo Model [5]	Developed by taking capillary tube as a starting point and assuming hydrate coats the walls of the tube	Simple	One empirical parameter. Ignores gas flow. Ignores other patterns to growth of hydrate. Ignores heterogeneity in pore shape and size distribution
Kleinberg Model [6]	Developed using fluid flux through capillary and by assigning specific patterns to growth of hydrate	Includes hydrate growth patterns. No empirical parameters	Ignores gas flow. Ignores heterogeneity in pore shape and size distribution
Daigle Model [7]	Developed using critical path analysis. Does not assume any hydrate growth pattern	Includes parameters that account for pore size and structure	Several empirical parameters. Does not account for fluid properties. Does not differentiate between gas and water. Ignores patterns of hdyrate growth
NRP (this study)	Developed using Navier Stokes equation for three-phase flow. Assumes hydrate growth within pore center and as coating on pore wall	Includes three phases. No empirical parameters. Includes different pore shapes and combination hydrate growth patterns	Ignores heterogeneity in pore size distribution

Figure 5 shows the comparison between the predictions from our model and the predictions from the other three models. The black and red legend show the relative permeability of water from our model with no irreducible water saturation when hydrates occupy the pore center and when hydrates coat the pore wall, respectively. While, the green and blue legend show the relative permeability of water with 20% irreducible water saturation when hydrates occupy the pore center and when hydrates coat the pore wall, respectively. It is clear that the first two models by Masuda et al. [5] and by Kleinberg et al. [6] do not allow any provision for irreducible water saturation such that the relative permeability from their model is much higher than other two models. Although, the model by Daigle [7] is able to able to account for the effect of non-zero S_{wr}, it is done using an empirical parameter called percolation threshold (p_c) that is analogous to irreducible water saturation in its physical meaning. Additionally, the model by Daigle [7] is based on few other empirical parameters that would require several experimental investigations to estimate their values. Nevertheless, having more empirical parameters would allow the model by Daigle [7] to obtain a better match with any experimental data. Our model (solid red line) is able to match the estimate from

Daigle [7] (dashed green line) without using any empirical parameter for values of S_{wr} and R that is similar to their analogous parameters p_c and r_{max}, respectively, in Daigle [7].

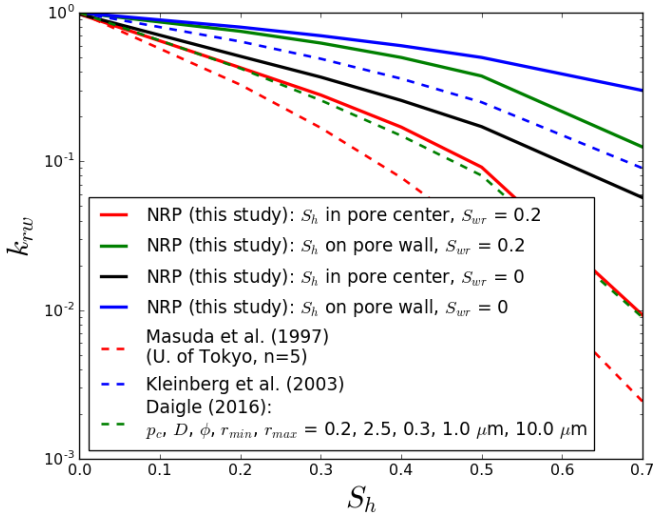

Figure 5: Comparison of water relative permeability vs. hydrate saturation as estimated by two popular models, a most recent model, and NRP (this study)

3.3. Water and Gas Relative Permeabilities from NRP

All the existing relative permeability models for hydrate bearing sediments provide an estimate of just water relative permeability. However, NRP, in addition to being fully non-empirical, is able to predict both the gas and the water relative permeability for hydrate bearing sediments of different growth patterns. Here, we illustrate the capability of NRP by estimating relative permeability of gas and water for different growth patterns of hydrate (i. pore filling, ii. wall coating, and iii. a combination of partially pore filling and partially wall coating) and for different pore shapes (i. cylindrical, ii. square, and iii. equilateral). For the results shown here, we assume non-zero irreducible water saturation ($S_{wr} = 0.2$). Figure 6 shows the results for $(k_{rw})_{eff}$ and $\left(k_{rg}\right)_{eff}$ with varying hydrate saturation as estimated by NRP (this study) for three different pore shapes (i. cylindrical, ii. square, and iii. equilateral) and four different hydrate growth patterns (i. wall coating, ii. 30 % pore filling, 70 % wall coating, iii. 70 % pore filling, 30 % wall coating, and iv. pore filling). Detailed results for $(k_{rw})_{eff}$ and $\left(k_{rg}\right)_{eff}$ as a function of S_w and S_h are presented in Appendix B.

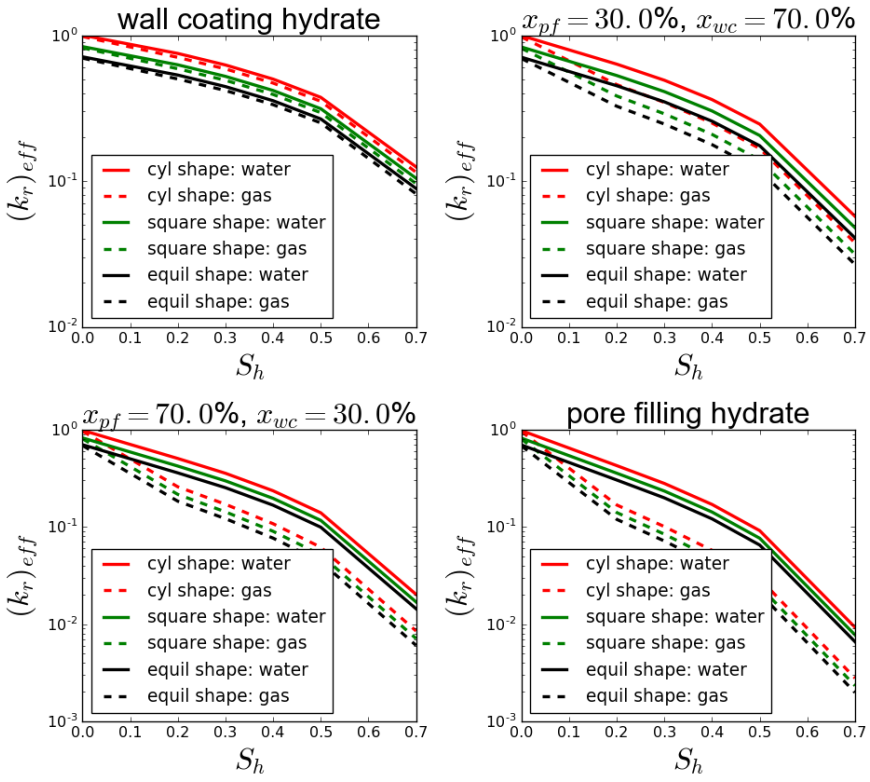

Figure 6: $(k_{rw})_{eff}$ and $(k_{rg})_{eff}$ vs. S_h as estimated by NRP (this study) for three different pore shapes (i. cylindrical, ii. square, and iii. equilateral) and four different hydrate growth pattern.

3.4. Effect of Pore Shapes

From Figure 6, it can be seen that irrespective of the type of hydrate growth pattern, $(k_{rw})_{eff}$ and $(k_{rg})_{eff}$ are largest for cylindrical pore shapes followed by square and equilateral triangle shaped pores, respectively. Similar observation was reported by Dai and Seol [19] using a pore scale study. It is also apparent from this figure that the effect of pore shapes on relative permeability decreases as hydrate occupies the pore center or when majority of the pore space is filled with hydrate saturation for any pattern of hydrate growth. The effect of pore shapes is similar on both water and gas. The reason why $(k_r)_{eff}$ is less than 1 for non-cylindrical pore shapes is because of their relative decrease in relative permeability as a result of their shapes. Although the relative permeability for the other pore shapes are shown in reference to cylindrical pore shape, these relative permeability can be easily shown in absolute terms by moving their reference value to 1 at $S_h = 0$. Similar convention of cylindrical pore shape as reference for other pore shapes is adopted in results presented in Appendix B.

3.5.Effect of Hydrate Growth Pattern

From Figure 6, it can be seen that irrespective of the type of pore shape, $(k_{rw})_{eff}$ and $(k_{rg})_{eff}$ are largest for wall coating hydrates and they decrease in magnitude as more and more hydrate starts to occupy pore center, i.e., the permeability reduction is the largest in the case of hydrates occupying pore center.

Additionally, the change in hydrate growth pattern from wall coating to pore filling affects $(k_{rg})_{eff}$ relatively much more than $(k_{rw})_{eff}$.

4. SUMMARY AND CONCLUSIONS

At present, there are two types of relative permeability models that are used to model gas production from hydrate-bearing sediments, i) fully empirical parameter fitting models (van Genuchten, Brooks Corey etc.), ii) Kozeny-Carman and capillary tube based models that assume only water as the mobile phase. This study proposed an analytical model based on fundamental principles of multiphase fluid flow to estimate relative permeability of both gas and water as a function of three phase saturations (hydrate, gas, water) and fluid properties. The proposed model is free of any empirical parameters and, therefore, does not require experimental data. Our model can account for different patterns of hydrate growth (i. pore filling, ii. wall coating, and iii. combination of partially pore filling and partially wall coating) and it can also account for heterogeneity in pore shapes. Since the model uses only the fluid and rock parameters, it can be used to obtain important physical parameters (for e.g. S_{wr}) by history matching laboratory data.

We estimated relative permeability for gas and water by using NRP for different pore shapes and different patterns of hydrate growth. Results suggest that the relative permeability for both gas and water is largest for cylindrical pore shapes followed by square and equilateral triangle shaped pores, respectively. However, the effect of pore shape tends to subside as hydrate occupies the pore center or when majority of the pore space is occupied with hydrate saturation for any pattern of hydrate growth. We also observe that relative permeability for both gas and water is largest for wall coating hydrates and it decreases in magnitude as more and more hydrate starts to occupy pore center, i.e., the permeability reduction is the largest in the case of hydrates occupying pore center.

One of the assumptions in the proposed model is negligible capillary pressure between gas and water. Our future study will consider the effect of capillary pressure in addition to testing of the model using a more comprehensive relative permeability dataset from our ongoing in-house experiments.

Acknowledgment

This technical effort was performed in support of the National Energy Technology Laboratory's ongoing research under the RES contract DE-FE0004000. This research was supported in part by an appointment to the National Energy Technology Laboratory Research Participation Program, sponsored by the U.S. Department of Energy and administered by the Oak Ridge Institute for Science and Education

REFERENCES

[1] M. L. Delli and J. L. H. Grozic, "Experimental determination of permeability of porous media in the presence of gas hydrates," *Journal of Petroleum Science and Engineering*, vol. 120, pp. 1–9, Aug. 2014.

[2] A. Johnson, S. Patil, and A. Dandekar, "Experimental investigation of gas-water relative permeability for gas-hydrate-bearing sediments from the Mount Elbert Gas Hydrate Stratigraphic Test Well, Alaska North Slope," *Marine and Petroleum Geology*, vol. 28, no. 2, pp. 419–426, Feb. 2011.

[3] A. Kumar, B. Maini, P. R. Bishnoi, M. Clarke, O. Zatsepina, and S. Srinivasan, "Experimental determination of permeability in the presence of hydrates and its effect on the dissociation characteristics of gas hydrates in porous media," *Journal of Petroleum Science and Engineering*, vol. 70, no. 1–2, pp. 114–122, Jan. 2010.

[4] H. Liang, Y. Song, Y. Chen, and Y. Liu, "The Measurement of Permeability of Porous Media with Methane Hydrate," *Petroleum Science and Technology*, vol. 29, no. 1, pp. 79–87, Jan. 2011.

[5] Y. Masuda, S. Naganawa, S. Ando, and K. Sato, "Numerical calculation of gas-production performance from reservoirs containing natural gas hydrates," in *SPE Asia Pacific Oil and Gas Conference*, 1997, pp. 14–17.

[6] R. L. Kleinberg *et al.*, "Deep sea NMR: Methane hydrate growth habit in porous media and its relationship to hydraulic permeability, deposit accumulation, and submarine slope stability," *J. Geophys. Res.*, vol. 108, no. B10, p. 2508, Oct. 2003.

[7] H. Daigle, "Relative permeability to water or gas in the presence of hydrates in porous media from critical path analysis," *Journal of Petroleum Science and Engineering*, vol. 146, pp. 526–535, Oct. 2016.

[8] J. Cai, E. Perfect, C.-L. Cheng, and X. Hu, "Generalized Modeling of Spontaneous Imbibition Based on Hagen–Poiseuille Flow in Tortuous Capillaries with Variably Shaped Apertures," *Langmuir*, vol. 30, no. 18, pp. 5142–5151, May 2014.

[9] A. C. M. Franken, J. A. M. Nolten, M. H. V. Mulder, D. Bargeman, and C. A. Smolders, "Wetting criteria for the applicability of membrane distillation," *Journal of Membrane Science*, vol. 33, no. 3, pp. 315–328, Oct. 1987.

[10] D. R. Murray *et al.*, "Saturation, Acoustic Properties, Growth Habit, and State of Stress of a Gas Hydrate Reservoir from Well Logs," *Petrophysics*, vol. 47, no. 02, Apr. 2006.

[11] R. Coates, M. Kane, C. Chang, C. Esmersoy, M. Fukuhara, and H. Yamamoto, "Single-well Sonic Imaging: High-Definition Reservoir Cross-sections from Horizontal Wells," presented at the SPE/CIM International Conference on Horizontal Well Technology, 2000.

[12] H. Singh, "Representative Elementary Volume (REV) in Spatio-Temporal Domain: A Method to find REV for Dynamic Pores," *Journal of Earth Science*, no. In press, 2017.

[13] Singh and S. Srinivasan, "Scale up of Reactive Processes in Heterogeneous Media - Numerical Experiments and Semi-analytical Modeling," presented at the SPE Improved Oil Recovery Symposium, Tulsa, Oklahoma, USA, 2014.

[14] H. Singh and S. Srinivasan, "Some perspectives on Scale-up of Flow and Transport in Heterogeneous Media," *Bulletin of Canadian Petroleum Geology*, 2014.

[15] J. L. Jensen and I. D. Currie, "A New Method for Estimating the Dykstra-Parsons Coefficient To Characterize Reservoir Heterogeneity," *SPE Reservoir Engineering*, vol. 5, no. 03, pp. 369–374, Aug. 1990.

[16] J. Jensen, D. Hinkley, and L. Lake, "A Statistical Study of Reservoir Permeability: Distributions, Correlations, and Averages," *SPE Formation Evaluation*, vol. 2, no. 4, Dec. 1987.

[17] L. Fenton, "The Sum of Log-Normal Probability Distributions in Scatter Transmission Systems," *IRE Transactions on Communications Systems*, vol. 8, no. 1, pp. 57–67, 1960.

[18] H. Singh, F. Javadpour, A. Ettehadtavakkol, and H. Darabi, "Nonempirical Apparent Permeability of Shale," *SPE Reservoir Evaluation & Engineering*, vol. 17, no. 03, pp. 414–424, Aug. 2014.
[19] S. Dai and Y. Seol, "Water permeability in hydrate-bearing sediments: A pore-scale study," *Geophys. Res. Lett.*, vol. 41, no. 12, p. 2014GL060535, Jun. 2014.

APPENDIX A: ADDITIONAL MODEL INFORMATION

A.1. Hydrates Occupying Pore Center

A.1.1. System of equations:

$$c_1 \ln(r_h) + c_2 = -c_g r_h^2 \quad (54)$$
$$c_1 \ln(r_g) + c_2 - c_3 \ln(r_g) - c_4 = (c_w - c_g) r_g^2 \quad (55)$$
$$\alpha c_1 - c_3 = 2 r_g^2 (c_w - \alpha c_g) \quad (56)$$
$$c_3 \ln(r_w) + c_4 = -c_w r_w^2 \quad (57)$$

A.1.2. Saturations of hydrate, gas, water:

$$S_h = \frac{\pi r_h^2 L}{\pi R^2 L} = \frac{r_h^2}{R^2} \quad (58)$$

$$S_g = \frac{r_g^2 - r_h^2}{R^2} \quad (59)$$
$$S_w = \frac{R^2 - r_g^2}{R^2} \quad (60)$$

$$\Rightarrow r_h = R\sqrt{S_h} \quad (61)$$

$$\Rightarrow r_g = R\sqrt{S_h + S_g} \quad (62)$$

$$\Rightarrow r_w = R\sqrt{1 - S_{wr}} \quad (63)$$

A.2. Hydrates Coating Pore Wall

A.2.1. System of equations:

$$c_1 = 0 \quad (64)$$
$$c_2 - c_3 \ln(r_g) - c_4 = (c_w - c_g) r_g^2 \quad (65)$$
$$c_3 = 2 r_g^2 (\alpha c_g - c_w) \quad (66)$$
$$c_3 \ln(r_w) + c_4 = -c_w r_w^2 \quad (67)$$

A.2.2. Saturations of hydrate, gas, water:

$$S_g = \frac{r_g^2}{R^2} \quad (68)$$
$$S_w = \left[\frac{(r_w^2 - r_g^2)}{R^2} + S_{wr}\right] \quad (69)$$
$$S_h = 1 - S_g - S_w = 1 - \frac{r_g^2}{R^2} - \left[\frac{(r_w^2 - r_g^2)}{R^2} + S_{wr}\right] \quad (70)$$

$$\Rightarrow r_g = R\sqrt{S_g} \tag{71}$$

$$\Rightarrow r_w = R\sqrt{S_g + (S_w - S_{wr})} \tag{72}$$

$$\Rightarrow r_w = R\sqrt{1 - S_h - S_{wr}} \tag{73}$$

APPENDIX B: ADDITIONAL RESULTS

B.1. NRP for Cylindrical Shaped Pores

B.1.1. Hydrates Occupying Pore Center

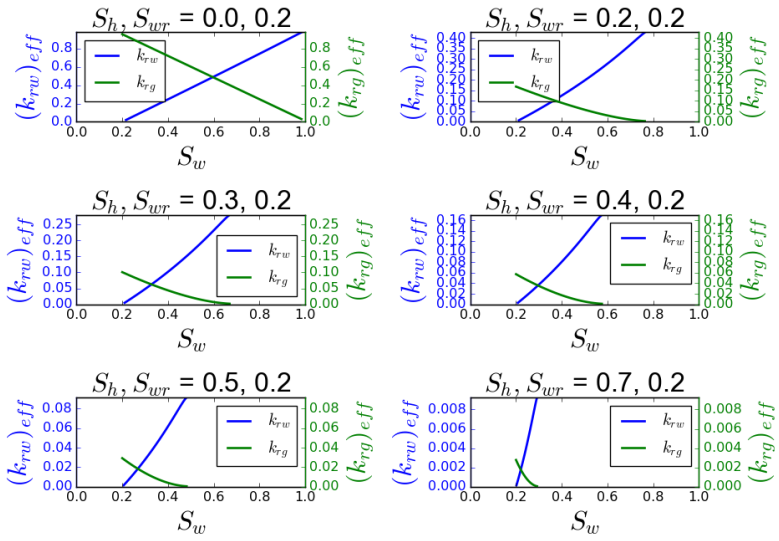

Figure 7: k_{rg} and k_{rw} for different S_h with hydrate occupying pore center

B.1.2. Hydrates Coating Pore Wall

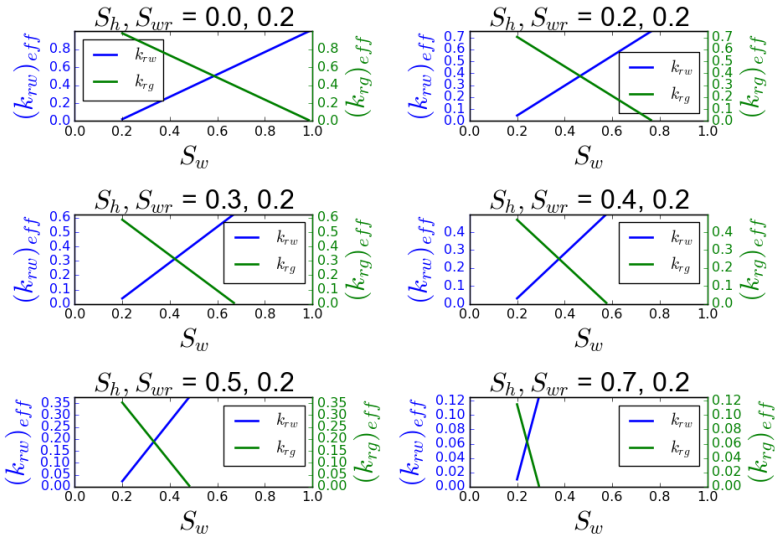

Figure 8: k_{rg} and k_{rw} for different S_h with hydrate coating the pore wall

B.1.3. Hydrates Partially Occupying Pore Center and Partially Coating Pore Wall

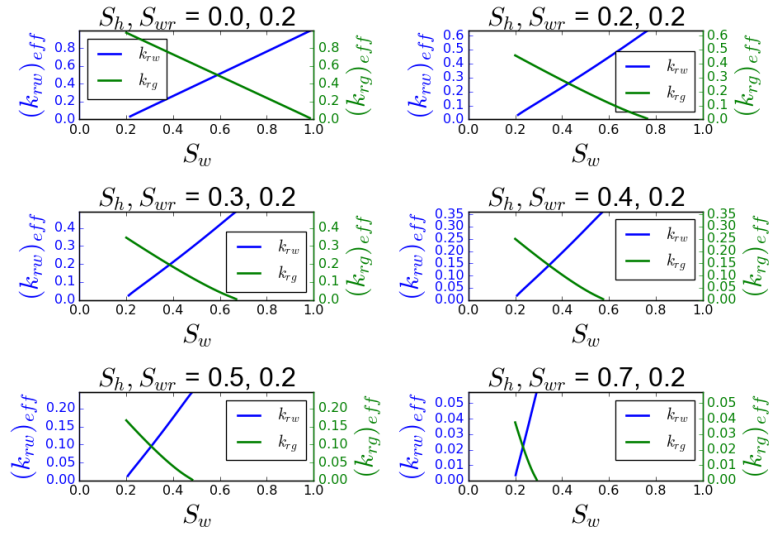

Figure 9: k_{rg} and k_{rw} for different S_h with hydrate partially occupying pore center (30 %) and partially coating the pore wall (70 %)

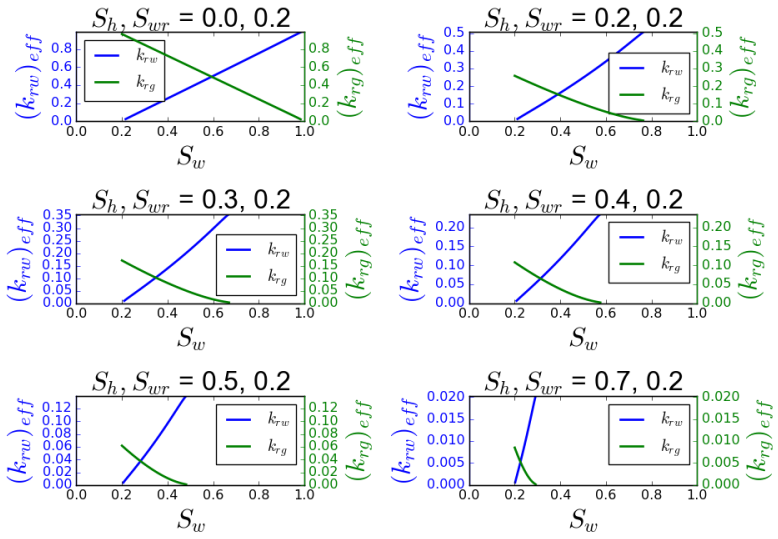

Figure 10: k_{rg} and k_{rw} for different S_h with hydrate partially occupying pore center (70 %) and partially coating the pore wall (30 %)

B.2. NRP for Square Shaped Pores

B.2.1. Hydrates Occupying Pore Center

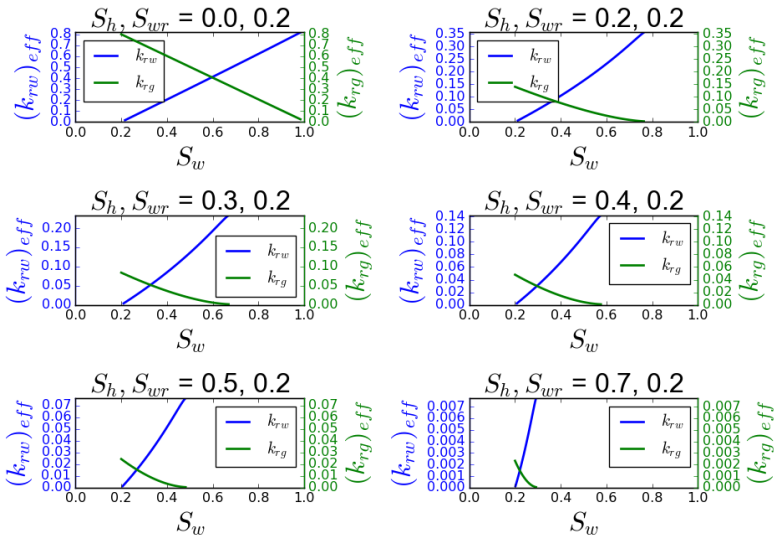

Figure 11: k_{rg} and k_{rw} for different S_h with hydrate occupying pore center

B.2.2. Hydrates Coating Pore Wall

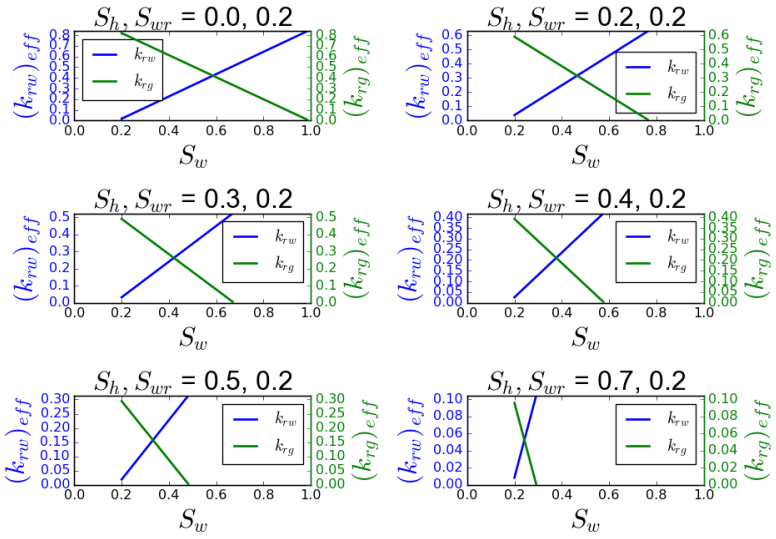

Figure 12: k_{rg} and k_{rw} for different S_h with hydrate coating the pore wall

B.2.3. Hydrates Partially Occupying Pore Center and Partially Coating Pore Wall

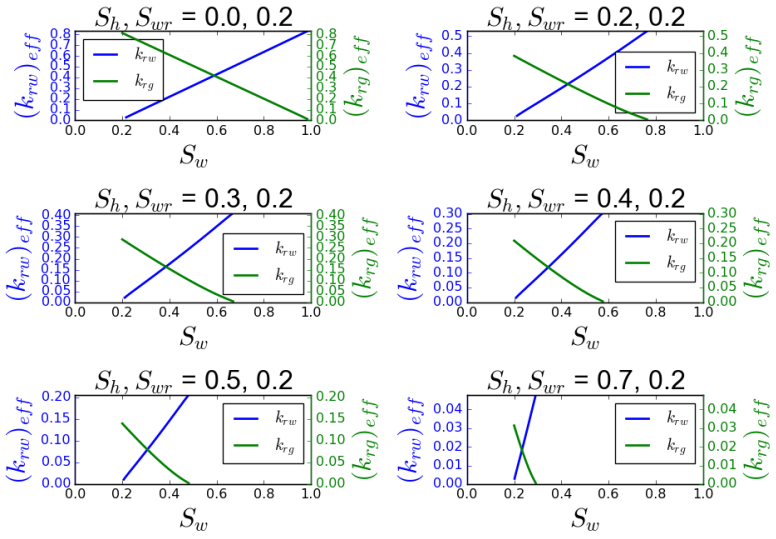

Figure 13: k_{rg} and k_{rw} for different S_h with hydrate partially occupying pore center (30 %) and partially coating the pore wall (70 %)

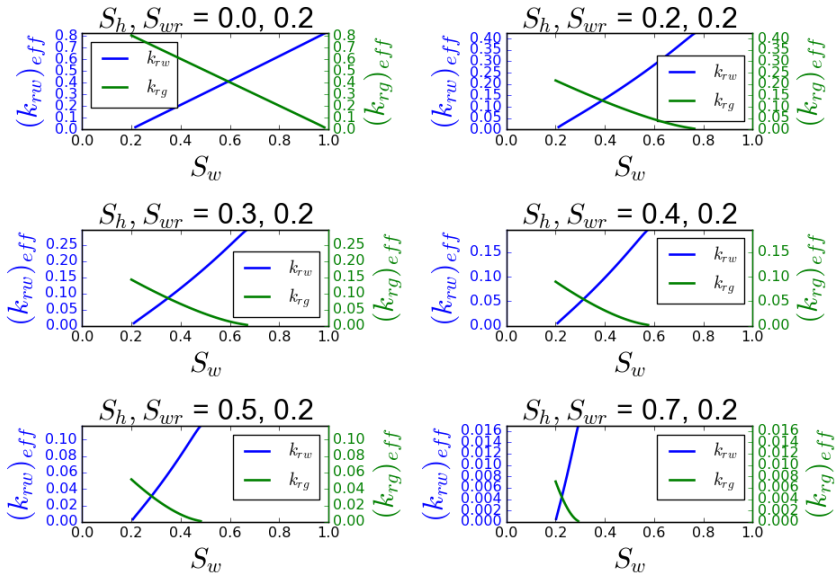

Figure 14: k_{rg} and k_{rw} for different S_h with hydrate partially occupying pore center (70 %) and partially coating the pore wall (30 %)

B.3. NRP for Equilateral Triangle Shaped Pores

B.3.1. Hydrates Occupying Pore Center

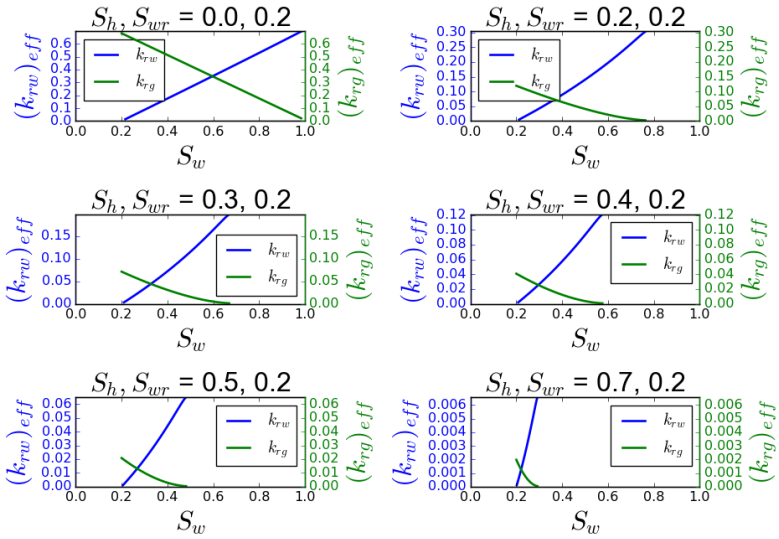

Figure 15: k_{rg} and k_{rw} for different S_h with hydrate occupying pore center

B.3.2. Hydrates Coating Pore Wall

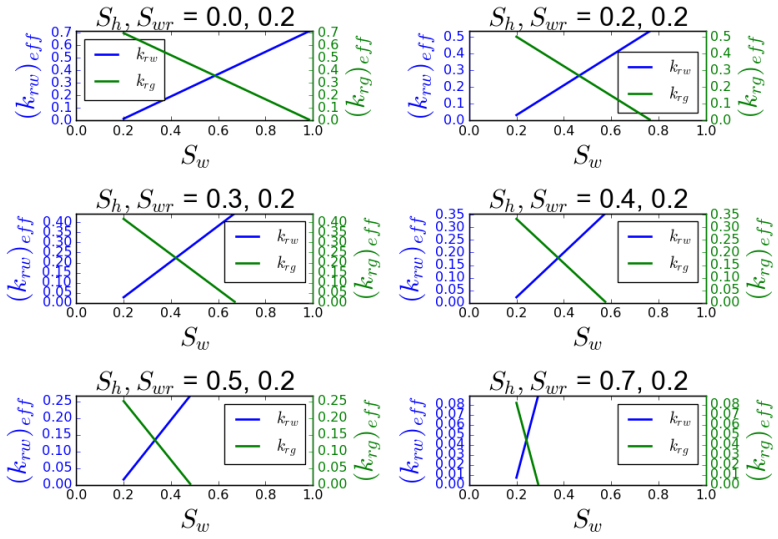

Figure 16: k_{rg} and k_{rw} for different S_h with hydrate coating the pore wall

B.3.3. Hydrates Partially Occupying Pore Center and Partially Coating Pore Wall

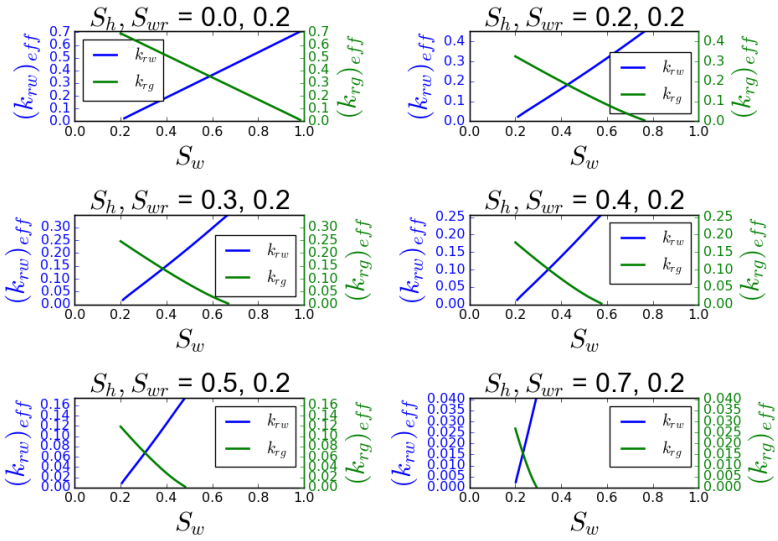

Figure 17: k_{rg} and k_{rw} for different S_h with hydrate partially occupying pore center (30 %) and partially coating the pore wall (70 %)

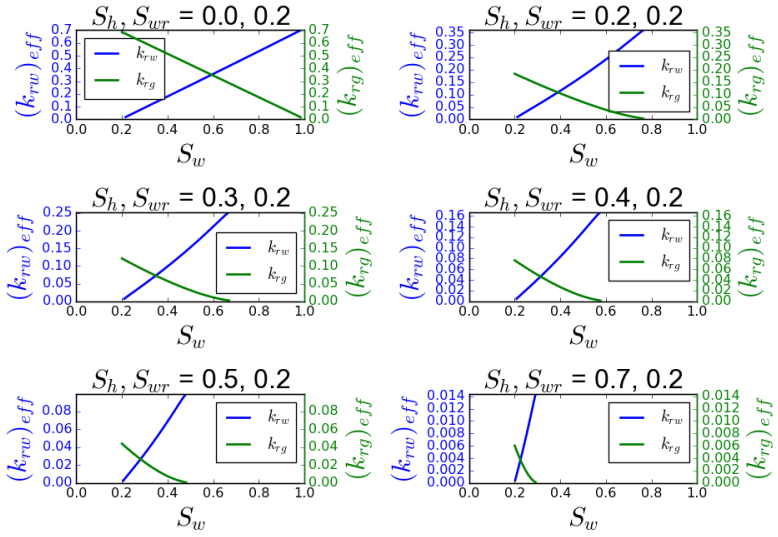

Figure 18: k_{rg} and k_{rw} for different S_h with hydrate partially occupying pore center (70 %) and partially coating the pore wall (30 %)